

An Analytical Approach for Continuous-Thrust, LEO-Molniya Transfers

David B. Spencer* and Felix Acon-Chen†

The Pennsylvania State University, University Park, PA 16802

This paper presents a comparison between an analytical approximation to a spacecraft transfer from a low Earth orbit to a highly elliptical Molniya orbit with an optimal solution. In this paper, a spacecraft is transferred from low Earth orbit to the final mission orbit by using various initial thrust accelerations ranging from 10^{-1} to 10^{-2} m/sec². An approximate analytical method using a blended control that satisfy some basic physical constraints on the orbit transfer and comparing these results to the exact optimal case found using a well known trajectory optimization software. The comparison between the analytical data and the numerical data showed that the percent error between the two is small, there is about a 13% percent difference in propellant usage for the initial thrust acceleration of 10^{-1} m/sec² and 10^{-2} m/sec². The factor that affected the results of both solutions is that in the analytical method, the radius of perigee was held constant while with the numerical solution the radius of perigee was free. This difference indicates that while the analytical solution was closely related to numerical solution, it can be improved by doing another analytical analysis with the radius of perigee free.

Nomenclature

$a, e, i, \Omega, \omega, \nu$	= Classical orbital elements
p, f, g, h, k, L	= Equinoctial orbital elements
a	= Semimajor axis, km
e	= Eccentricity
g_0	= Gravitational acceleration at sea level, m/sec ²
i	= Inclination, deg
I_{sp}	= Specific impulse, sec
L	= Argument of longitude, deg
m	= Mass, kg
M	= Mean anomaly, deg
P	= Power, kW
R_{Earth}	= Radius of Earth, km
t	= Time, hrs
T	= Thrust, N
\vec{T}	= Thrust vector, N
α	= In-plane control angle, deg
β	= Out-of-plane control angle, deg
ΔV_{eff}	= Effective change in velocity, m/sec

* Assistant Professor, Department of Aerospace Engineering, 229 Hammond Building. Associate Fellow, AIAA

† Undergraduate Research Assistant, Department of Aerospace Engineering, 229 Hammond Building. Student Member, AIAA.

$\Delta_r, \Delta_\theta, \Delta_n$	= Radial, tangential, and normal thrust acceleration, N/kg
Δt	= Change in time
ε	= Power efficiency
μ	= Gravitational constant, km ³ /sec ²
η	= Non-dimensional mass ratio
ν	= True anomaly, deg
Ω	= Right ascension of the ascending node, deg
ω	= Argument of periaipse, deg

Subscripts

initial or 0	= Initial value
final	= Final value

I. Introduction

During the past few decades, various groups have attempted to develop a solar-electric-propulsion spacecraft, since such a vehicle would have a significantly increased propellant efficiency, greater maneuverability, larger payload capabilities, and a greater lifetime than a conventional chemical-propulsion space vehicle¹. Many studies have been conducted in an attempt to find the best method for computing an optimal low-thrust Earth-orbit transfer.

Previously, the trajectory optimization problem regarding the low-thrust propulsion systems has been investigated in order to find the best solution method. For example, multiple optimal and non-optimal transfer trajectories between specific initial and final orbits have been studied². In addition, a method of averaging that provides a quick trajectory evaluation compared to methods based upon numerical integration of differential equations was developed³.

In another study, Lawden's "primer vector" theory was used to analyze impulsive and near-impulsive transfers in order to predict the conditions for low-thrust transfers. This study used algebraic approximations to compute the total time and gravity loss for relatively efficient transfers and to demonstrate that gravity losses for a transfer are reduced to a low level if enough burns are done⁴.

Herman and Conway⁵ found optimal, low-thrust, Earth-moon orbit transfers by applying a method of collocation with nonlinear programming. The Earth orbit of the spacecraft and the final lunar orbit are both arbitrary while the moon is in its actual orbit. Furthermore, the total transfer time is minimized, but the trajectory is also propellant minimizing since the propulsion system operates continuously and prohibits a coast arc. They also discovered that a very low initial thrust acceleration of 10⁻⁴ g yields flight times of approximately 32 days and requires many revolutions of both the Earth and the moon. In addition, if the problem is solved as two coupled two-body problems by ignoring the third body, then the optimal trajectory is changed slightly. The optimal trajectory is also insensitive to change in the engine specific impulse as long as the same initial thrust acceleration magnitude is used.

On the other hand, Prussing⁶ examined minimum-fuel impulsive spacecraft trajectories in which long-duration coast arcs between thrust impulses are possible. If the coast time is long enough that it allows one or more complete revolutions of the central body then the solutions become

complicated. This type of scenario presents Lambert's problem in which the determination of the orbit that connects two specified terminal points in a specified time interval brings about multiple solutions; a transfer time long enough to allow N revolutions of the central body has $2N + 1$ trajectories that satisfy the boundary value problem. In order to solve all the trajectories, Prussing developed an algorithm based on the classical Lagrange formulation for an elliptic orbit. Moreover, this procedure is applied to the problem of rendezvous with a target in the same circular orbit as the spacecraft while the minimum-fuel optimality of the two-impulse trajectory is determined using primer vector theory⁶.

Kechichian⁷ also studied the minimum-time low-thrust rendezvous and transfer using the epoch mean longitude formulation. His study shows the state and adjoint differential equations as explicit functions of time that include natural orbital elements that stay constant if no perturbations are applied. In addition, the optimal Hamiltonian is time varying while the function that defines the transversality condition at the end time in minimum-time problems is illustrated as constant during the optimal transfer.

Coverstone-Carroll and Williams⁸ developed a direct optimization method based on differential inclusion concepts and used the formulation to compute low thrust trajectories. This procedure removes explicit control dependence from the problem statement which reduces the dimension of the parameter space and requires fewer nonlinear constraints in the resulting nonlinear programming problem. Moreover, the study presents simulations for a two-dimensional gravity-free trajectory which involves a maximum velocity transfer to a rectilinear path, an Earth-Mars constant specific impulse transfer, an Earth-Jupiter constant specific impulse transfer, and an Earth-Venus-Mars variable specific impulse gravity assist.

In another study, Betts⁹ used the direct transcription method, one of the most effective numerical techniques, to solve the trajectory optimization and optimal control problems. This method combines a sparse nonlinear programming algorithm with a discretization of the trajectory dynamics. Furthermore, the vehicle dynamics are defined by using a modified set of equinoctial coordinates while the trajectory modeling is described using these dynamics. Also, in order to demonstrate some special features of this method such as alternate coordinate systems during the transfer and mesh refinement to produce a high fidelity trajectory, the solution for the transfer from Earth to Mars including a swingby of the planet Venus is presented using the direct transcription method.

In addition, Kechichian¹⁰ explored the optimal low-Earth-orbit-Geostationary-Earth-orbit intermediate acceleration orbit transfer by analyzing the problem of minimum-time orbit transfer using intermediate acceleration through precision integration and averaging. In his study, continuous constant accelerations of the order of $10^{-2}g$ are considered for applications using nuclear propulsion upper stages; in addition, the acceleration vector is optimized in direction with its magnitude held constant throughout the flight. The scenarios examined have trajectories that circle the Earth for only a few orbits before reaching geostationary Earth orbit, and these trajectories have demonstrated to be sensitive to departure and arrival points, requiring the use of the full six-state dynamics for satisfactory and meaningful results. Also, the ΔV losses with respect to very low-acceleration transfers are shown to be small.

Herman and Spencer¹ focused on optimal low-thrust Earth-orbit transfers using higher-order collocation methods in which several Earth-orbit transfers, the LEO-to-GEO, LEO-to-MEO, and LEO-to-HEO transfers, were computed and then compared to the solutions found through analytical blended control methods. For each of these scenarios, a spacecraft is transferred from LEO to the final mission orbit by using various initial thrust accelerations (TA) ranging from 10^0 to 10^{-2} g. This study involved determining the control time histories of a set of states, a system of first-order ordinary differential equations, from specified initial conditions to the desired final conditions while minimizing a function of the final values of states and/or time. These time histories are determined through a performance function, a scalar function consisting of the values of the states at the final time and the initial and final times, which is minimized while meeting the initial and final conditions of the system of differential equations.

This paper discusses the solution to the optimal control problem using NASA's SEPSHOT software program on the LEO-to-Molniya transfer. An analytical formulation by Spencer¹¹ for a LEO-Molniya transfer is compared with the results obtained from the program. As the SEPSHOT software uses equinoctial elements in its computations, equinoctial elements are also used for the analytical study. All results are converted back into classical orbital elements to provide better physical insight of the results. The final data is analyzed and compare with the results in Spencer's analytical solutions. Overall, there are a total of five plots for each initial thrust acceleration (10^{-1} N/kg and 10^{-2} N/kg). For these graphs, the semimajor axis, eccentricity, inclination, apogee and perigee radius, and energy are all plotted versus time.

II. Analytical Solution Method

The analytical solution method minimizes the propellant usage for a given transfer by assuming that the propellant usage rate is constant during a burn, which means, the burn times for a given maneuver are minimized by maximizing the time rate of change of the particular orbital parameter that governs the burn. During the first burn, thrusting is performed in the orbit plane to increase the apogee radius to the desired final radius value. In addition, the rate of change of the semimajor axis, da/dt , is maximized by determining the in-plane (α) motion of the thrust direction. Also, during the first burn, the out-of-plane component of the thrust vector does not exist. Afterwards, a coast is initiated and lasts until there is a second burn¹.

For the second burn, the periapse is kept constant while the inclination is changed from the initial value to the desired final value by maximizing the time rate of change in inclination, di/dt . This results in the out-of-plane thrust angle (β) being near ± 90 degrees while the inclination change maneuver is centered about the apogee. Figure 1 illustrates the thrust vector and angle definitions¹.

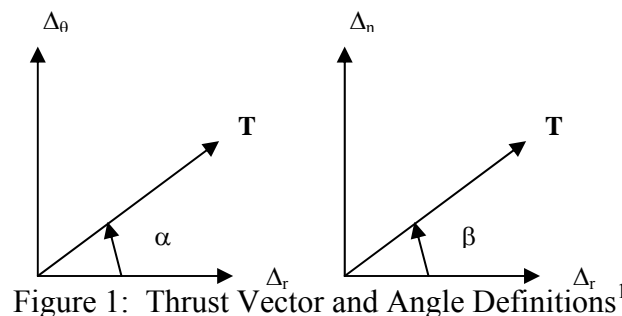


Figure 1: Thrust Vector and Angle Definitions¹

For various cases of the LEO-to-Molniya transfers with a range of TA values, a specific impulse of 1000 sec was used.

III. Analytical Solution Method Equations

In order to avoid the singularities that occur in the modified classical orbit elements (a, e, i, Ω, ω) when $e = 0$ and $i = 0$ deg, modified equinoctial orbit elements must be used to describe the orbit transfers¹. Therefore, the modified equinoctial orbit elements (p, f, g, h, k, L) must be defined in terms of the modified classical orbital elements as:

$$p = a(1 - e^2) \quad (1)$$

$$f = e \cos(\Omega + \omega) \quad (2)$$

$$g = e \sin(\Omega + \omega) \quad (3)$$

$$h = \tan \frac{i}{2} \cos \Omega \quad (4)$$

$$k = \tan \frac{i}{2} \sin \Omega \quad (5)$$

$$L = \Omega + \omega + \nu \quad (6)$$

The equations of motion of a thrusting spacecraft in an inverse square gravity field in terms of the modified equinoctial orbit elements are:

$$\frac{dp}{dt} = \left(\frac{2p}{w} \right) \left(\frac{p}{\mu} \right)^{\frac{1}{2}} \Delta_\theta \quad (7)$$

$$\frac{df}{dt} = \left(\frac{p}{\mu} \right)^{\frac{1}{2}} \left\{ \Delta_r \sin L + [(w+1) \cos L + f] \left(\frac{\Delta_\theta}{w} \right) - (h \sin L - k \cos L) \left(\frac{g \Delta_n}{w} \right) \right\} \quad (8)$$

$$\frac{dg}{dt} = \left(\frac{p}{\mu} \right)^{\frac{1}{2}} \left\{ -\Delta_r \cos L + [(w+1) \sin L + g] \left(\frac{\Delta_\theta}{w} \right) + (h \sin L - k \cos L) \left(\frac{f \Delta_n}{w} \right) \right\} \quad (9)$$

$$\frac{dh}{dt} = \left(\frac{p}{\mu} \right)^{\frac{1}{2}} \left(\frac{s^2 \Delta_n}{2w} \right) \cos L \quad (10)$$

$$\frac{dk}{dt} = \left(\frac{p}{\mu} \right)^{\frac{1}{2}} \left(\frac{s^2 \Delta_n}{2w} \right) \sin L \quad (11)$$

$$\frac{dL}{dt} = (\mu p)^{\frac{1}{2}} \left(\frac{w}{p} \right)^2 + \frac{1}{w} \left(\frac{p}{\mu} \right)^{\frac{1}{2}} (h \sin L - k \cos L) \Delta_n \quad (12)$$

$$\frac{dm}{dt} = -\frac{T}{c} \quad (13)$$

$$\frac{d\eta}{dt} = -\left(\frac{T}{m_0} \right) \left(\frac{1}{c} \right) \quad (14)$$

where $c = g_0 I_{sp}$, $w = 1 + f \cos L + g \sin L$, $s^2 = 1 + h^2 + k^2$ and $\eta = \frac{m}{m_0}$.

A measure of the total velocity change is found using the effective velocity, and is defined as

$$\Delta V_{eff} = - \left(\frac{T}{m_0} \right) \left\{ \frac{\ln[\eta(t_{final})] - \ln[\eta(t_{initial})]}{\eta(t_{final}) - \eta(t_{initial})} \right\} \Delta t \quad (15)$$

While the thrust vector \bar{T} is computed by using two angles α and β , which represent the in-plane and out-plane components of the thrust direction,

$$\bar{T} = T \begin{Bmatrix} \sin \alpha \cos \beta \\ \cos \alpha \cos \beta \\ \sin \beta \end{Bmatrix} = \begin{Bmatrix} \Delta_r \\ \Delta_\theta \\ \Delta_n \end{Bmatrix} \quad (16)$$

IV. Numerical Solution Method

The Fortran IV double precision version of NASA's SEPSHOT software is used in the numerical solution method. A costate formulation is used which results in a two point boundary value problem which is solved using a Newton iteration on the initial unknown parameters and the unknown transfer time. Also, a Runge-Kutta method is used to integrate the state and costate equations and averaging is done using a Gaussian quadrature^{12,13}.

SEPSHOT is designed to calculate time optimal or nearly time optimal geocentric transfers for a solar electric spacecraft with or without attitude constraints. The program has the option to use initial high thrust or low thrust. For the initial high thrust stage one or two impulses of fixed total ΔV can be included, and the initial orbit is assumed to be circular. For the low thrust stage, a nonsingular set of orbital elements and an averaging method are used. In addition, the low thrust phase is applicable to general geocentric elliptical orbits^{12,13}.

V. Numerical Solution Method Equations

A. Analytical Analysis of SEPSHOT's Results

Microsoft Excel was used to conduct an analytical analysis of all the data obtained from SEPSHOT. The data was plotted and then a polynomial trendline, a graphic representation of trends in data series, was added to each plot. To compute the trendline Microsoft Excel calculates the least squares fit through the data points by using the following equation where b and $c_1 \dots c_6$ are constants,

$$y = b + c_1 x + c_2 x^2 + c_3 x^3 + \dots + c_6 x^6 \quad (17)$$

A measure of how close the trendline is to the actual data is also conducted by computing the coefficient of determination, R^2 . The coefficient of determination is an indicator from 0 to 1 that reveals how closely the estimated values for the trendline correspond to the actual data. A trendline is most reliable when its R^2 value is at or near 1. R^2 is computed as follows:

$$R^2 = 1 - \frac{\sum (Y_j - \hat{Y}_j)^2}{\sum Y_j^2} \quad (18)$$

where the Y values correspond to the optimal values, and the \hat{Y} values correspond to the analytical values.

B. Initial Conditions

Tables 1 and 2 show the initial conditions required to run the computer simulation. The initial conditions used to declare the initial and final orbit consist of the semimajor axis, eccentricity, inclination, right ascension of the ascending node, and argument of perigee for both the LEO and Molniya orbits. In addition, the initial mass, initial power, thruster specific impulse, and efficiency are considered in order to compute the initial thrust acceleration using the following relation¹²⁻¹⁴:

$$P = \frac{g_0 T I_{SP}}{2\epsilon} \quad (19)$$

Also, the final conditions are the total effective change in velocity, the total transfer time (hours), the semimajor axis time history, the eccentricity time history, the inclination time history, the apogee and perigee radius time history, and the energy time history.

Table 1 Initial Conditions for the Initial and Final Orbit

Element	Initial Value (LEO)	Final Value (Molniya)
a	7,000 km	26,578 km
e	0	0.73646
i	28.5°	63.435°
Ω	0°	0°
ω	0°	0°

Table 2 Initial Conditions for Initial Thrust Acceleration

Element	TA = 10 ⁻¹ N/kg	TA = 10 ⁻² N/kg
Normalized Initial Mass (η)	1	1
P_0 (kw)	0.4905	0.04905
I_{SP} (sec)	1,000	1,000

VI. Results

A. LEO-Molniya Transfer: $T/m_0 = 10^{-1}$ N/kg

For the case of an initial thrust acceleration of 10⁻¹ N/kg, SEPSHOT accomplishes the transfer in one burn while achieving an overall effective change in velocity (ΔV) of 5,814.69 m/s in 12.18 hours. On the other hand, Spencer's analytical solution completes the transfer using two burns in 13.75 hours at a ΔV_{eff} of 6,896 m/s. Refer to Table 3 to view a comparison of the two solutions which shows that SEPSHOT's trajectory is slightly more efficient by completing the transfer in less time; in addition, there is a percent error of 12.89% between the numerical solution provided by SEPSHOT and Spencer's analytical solution.

Table 3 Initial Thrust Acceleration of 10^{-1} N/kg

	Overall Effective Change in Velocity (ΔV_{eff})	Overall Time	Percent Error (%)
Spencer's Results	6,896 m/s	13.75 hrs	12.89%
SESPOT's Results	5,814.69 m/s	12.18 hrs	

Five figures are now presented for this case. Figures 2-6 show a comparison of the time history of the semimajor axis, eccentricity, inclination, apogee and perigee radius, and energy between SESPOT's numerical data and Spencer's analytical data. A key aspect of the comparison that should be noticed is that SESPOT's trajectory manages to complete all the desired conditions in approximately the amount of time it takes Spencer's trajectory to complete the first burn.

Figure 2 shows how SESPOT manages to achieve a semimajor axis of 26,578 km (Molniya orbit) from a starting semimajor axis of 7,000 km (LEO Orbit) in 12.18 hours by using one burn. However, Spencer's trajectory shows that a burn is performed for approximately 12 hours, followed by a coast arc of 4.5 hours, and then a second burn is made which takes about 1.5 hours to complete the trajectory. One should also notice that SESPOT's trajectory seems almost parabolic while Spencer's trajectory has more of an oscillatory shape which could account for SESPOT's reduced time to complete the trajectory.

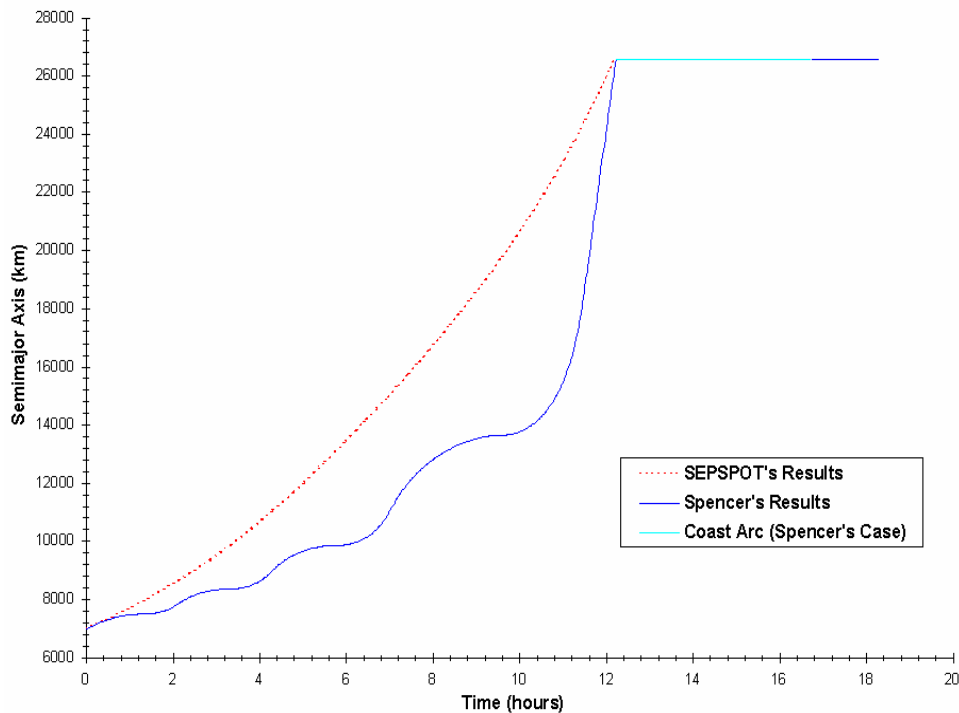


Figure 2: Semimajor Axis Time History, $T/m_0 = 10^{-1}$ N/kg

Figure 3 shows how Spencer's eccentricity curve slightly oscillates, but increases at a steady rate while SESPOT's curve increases slowly at the beginning and then the eccentricity starts increasing at a faster rate, resulting in a smooth parabolic curve. The oscillations in Spencer's trajectory could account for additional time required to achieve a final eccentricity of 0.73646.

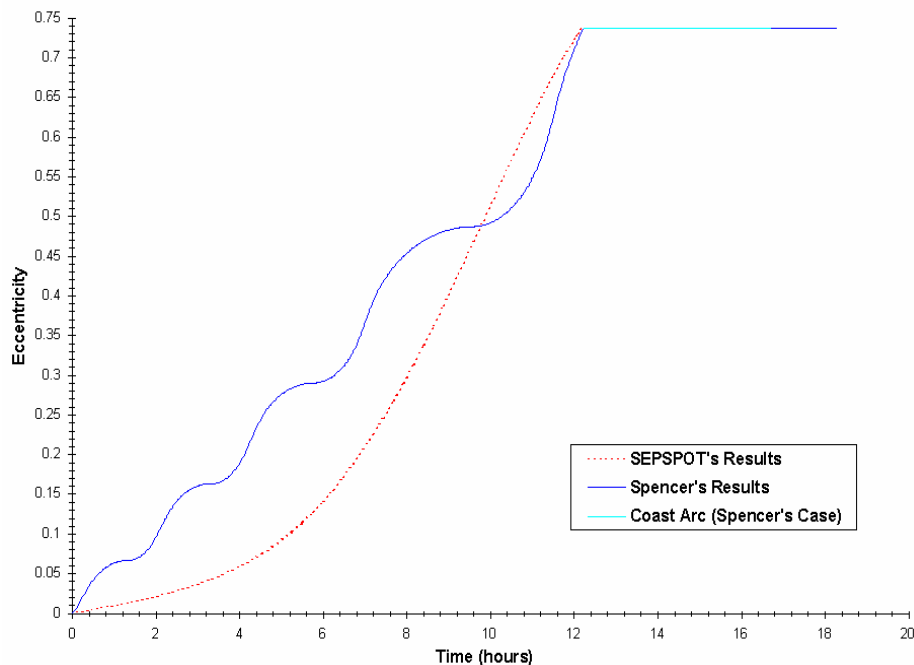


Figure 3: Eccentricity Time History, $T/m_0 = 10^{-1}$ N/kg

Figure 4 illustrates how for Spencer's results the angle of inclination stays constant at 28.5° during the first burn and then it rapidly increases to 63.435° in the second burn. SEPSPOt's results show how the angle of inclination is increased over time and a parabolic curve is formed.

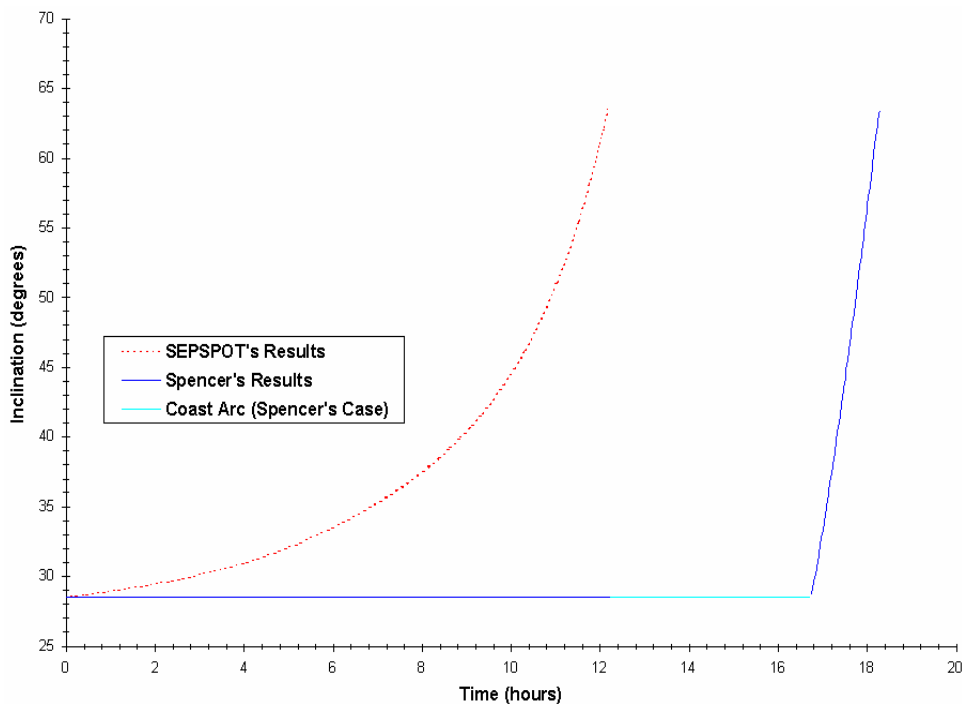


Figure 4: Inclination Time History, $T/m_0 = 10^{-1}$ N/kg

Figure 5 shows how SEPSHOT's trajectory achieves both the apogee and perigee radius desired conditions in the amount of time it takes Spencer's trajectory to complete the first burn. An important aspect of this plot is that SEPSHOT keeps the perigee radius free which forms a parabolic type curve while Spencer maintains a constant perigee radius. This is a key difference since it might account for the optimal trajectory found by SEPSHOT.

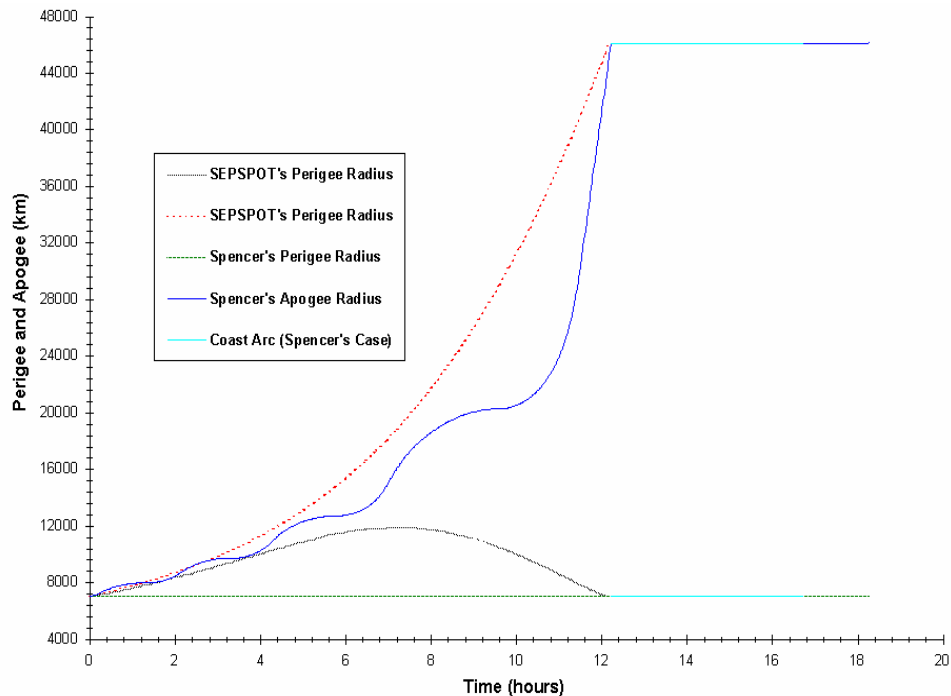


Figure 5: Apogee and Perigee Radius Time History, $T/m_0 = 10^{-1}$ N/kg

From Figure 6 one can see that SEPSHOT's trajectory achieves the energy levels required to complete the trajectory in less time. In addition, from the plot Spencer's data indicates that more energy is required to accomplish the desired LEO-Molniya transfer.

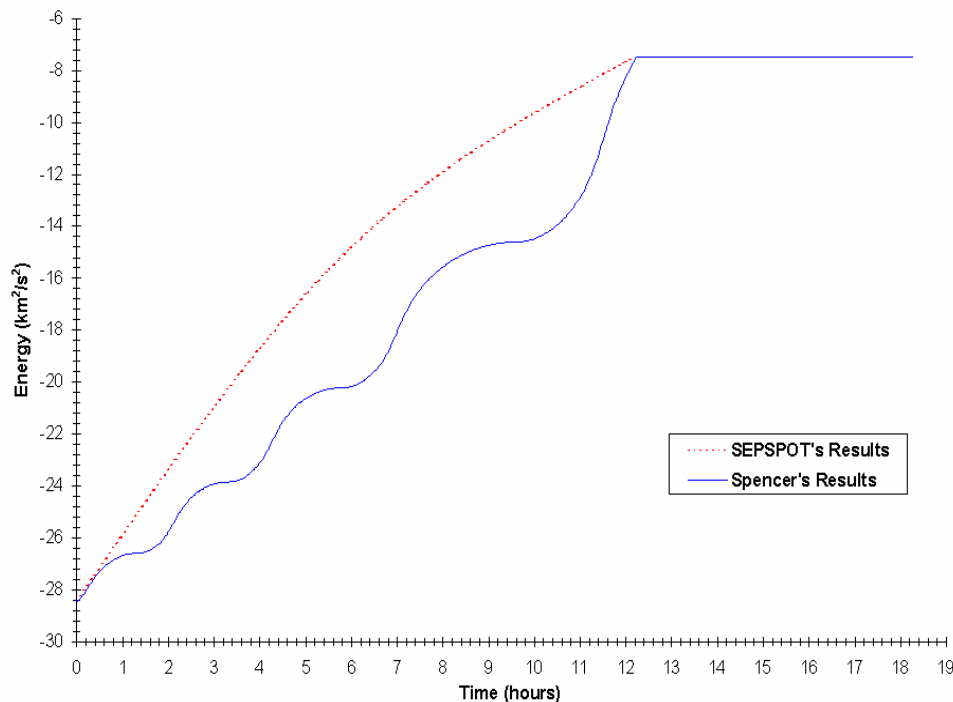


Figure 6: Energy Time History, $T/m_0 = 10^{-1}$ N/kg

In the case of an initial thrust acceleration of 10^{-2} N/kg, SEPSHOT completes the transfer in one burn while achieving a ΔV_{eff} of 5,814.69 m/s in 121.77 hours. Spencer's analytical solution achieves the transfer using one burn in 136.83 hours at a ΔV_{eff} of 6,844 m/s. Table 4 depicts a comparison of the two solutions in which SEPSHOT's trajectory is shown to be slightly more optimal by completing the transfer in less time. Furthermore, there is a percent error of 12.37% between the numerical solution provided by SEPSHOT and Spencer's analytical solution.

Table 4: Initial Thrust Acceleration of 10^{-2} N/kg

	Overall Effective Change in Velocity (ΔV_{eff})	Overall Time	Percent Error (%)
Spencer's Results	6,844 m/s	136.83 hrs	12.37%
SEPSHOT's Results	5,814.69 m/s	121.77 hrs	

Figures 7-11 illustrate a comparison of the time history of the semimajor axis, eccentricity, inclination, apogee and perigee radius, and energy between SEPSHOT's numerical data and Spencer's analytical data. One should note that unlike the previous case, both SEPSHOT's and Spencer's trajectories manage to achieve the desired orbit using only one burn.

Figure 7 shows that despite the fact that both trajectories only require one burn to complete the desired final conditions, Spencer's results are still taking longer to reach the final conditions. In this case SEPSHOT's semimajor axis curve is smooth and parabolic while Spencer's curve has a similar shape, but it contains small oscillations; these oscillations can account for the additional time required to reach the Molniya orbit.

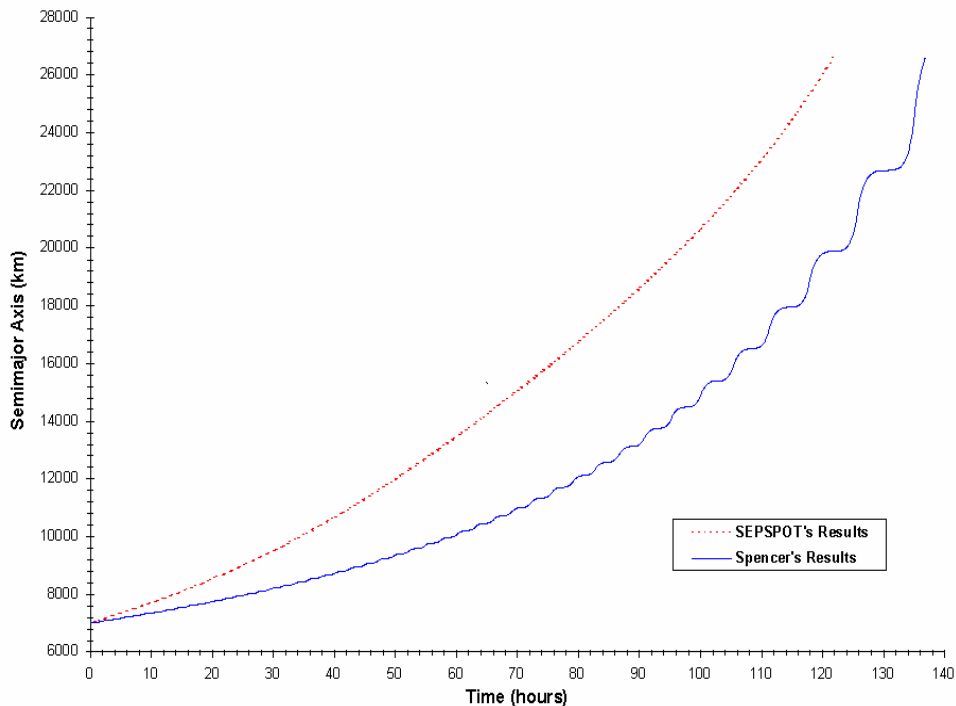


Figure 7: Semimajor Axis Time History, $T/m_0 = 10^{-2}$ N/kg

Figure 8 shows how for Spencer's results the eccentricity seems to increase at an almost constant rate with time. Furthermore, for SEPSHOT's results, like in previous initial thrust acceleration case, the curve increases slowly at the beginning and then the eccentricity starts increasing at a faster rate, resulting in a smooth parabolic curve.

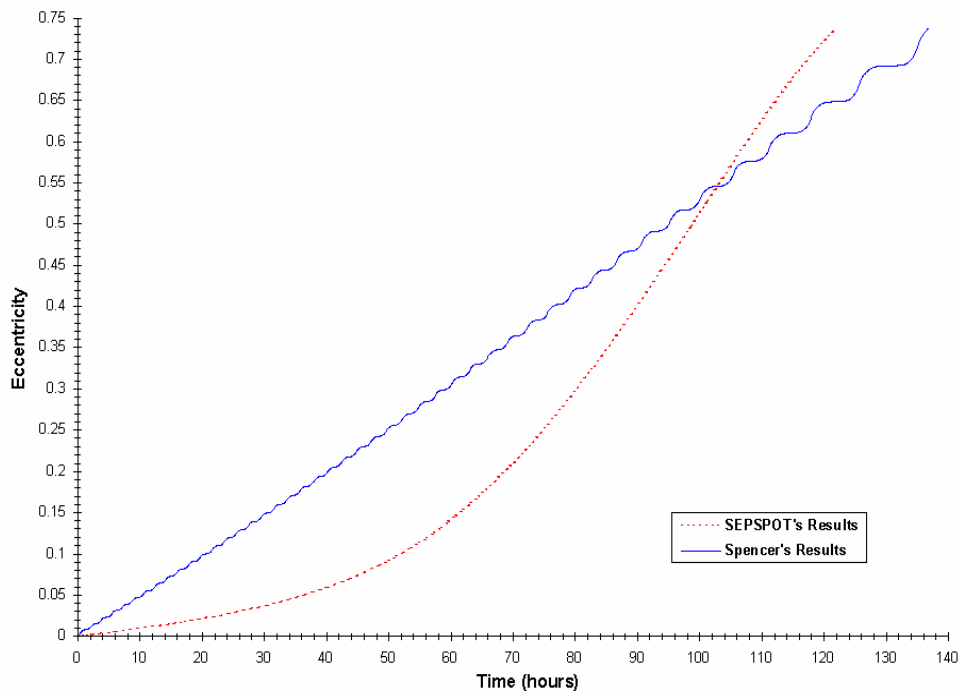


Figure 8: Eccentricity Time History, $T/m_0 = 10^{-2}$ N/kg

Figure 9 illustrates how for both Spencer's and SEPSOT's results, the angle of inclination is increased over time and a parabolic curve is formed. The only difference is that SEPSOT's curve is smooth while Spencer's curve has oscillations. In addition, the plot depicts how the angle of inclination for SEPSOT's trajectory increases at a much faster rate than Spencer's trajectory, hence reaching the desired angle of inclination in less time.

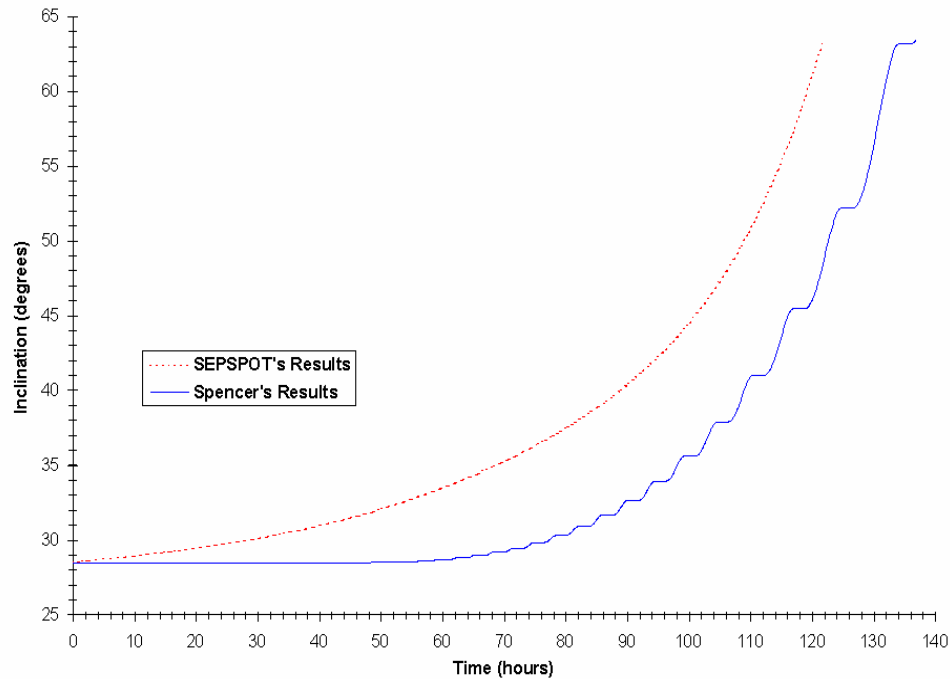


Figure 9: Inclination Time History, $T/m_0 = 10^{-2}$ N/kg

Figure 10 illustrates how SEPSOT keeps the perigee radius free and forms a parabolic type curve while Spencer maintains a constant perigee radius. This is a key difference since it might account for SEPSOT's more efficient trajectory.

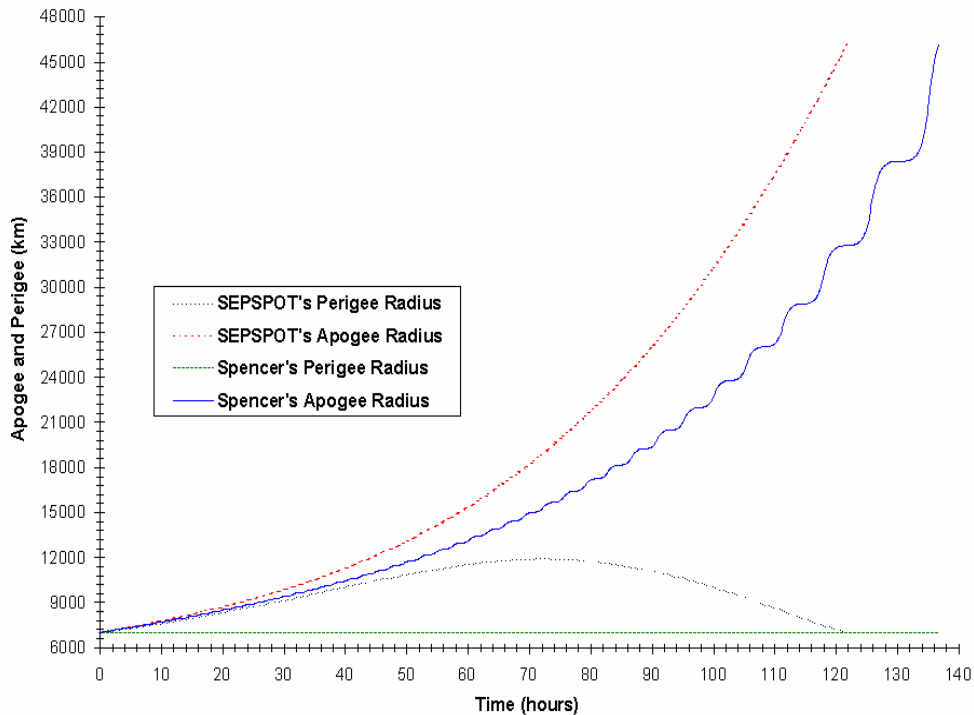


Figure 10: Apogee and Perigee Time History, $T/m_0 = 10^{-2}$ N/kg

Figure 11 shows how SEPSPOT's trajectory achieves the energy levels required to complete the trajectory in less time. In addition, from the plot Spencer's data indicates that more energy is required to accomplish the desired LEO-Molniya transfer.

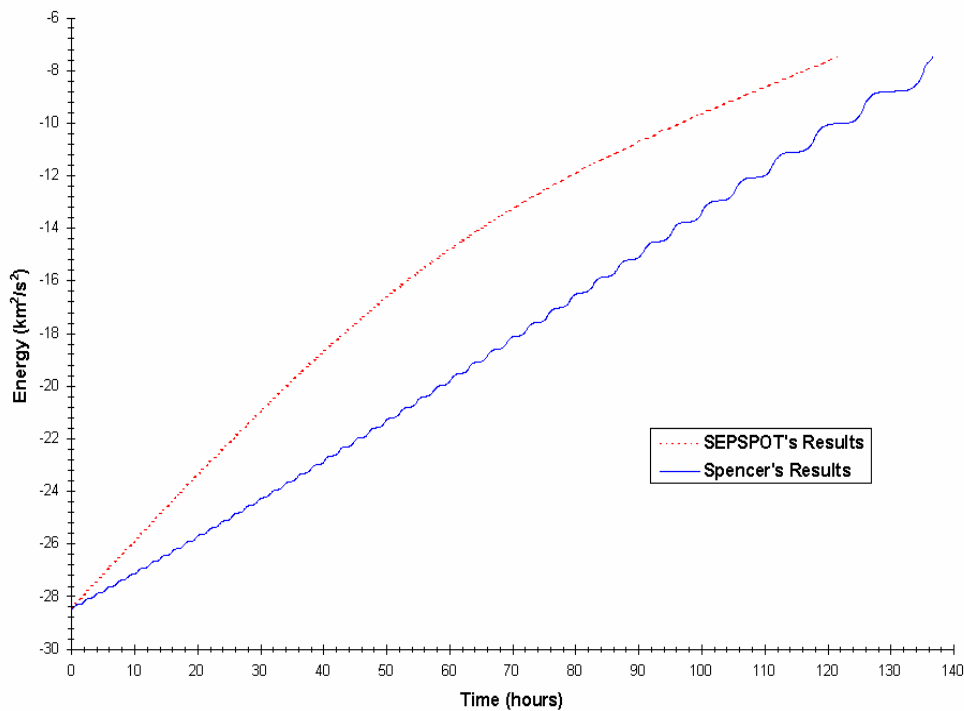


Figure 11: Energy Time History, $T/m_0 = 10^{-2}$ N/kg

An analytical analysis was performed on the time history of the semimajor axis, eccentricity, inclination, and equinoctial orbital elements. Table 5 shows the coefficients of the polynomial equation derived for each equinoctial orbital element (semimajor axis is used for the distance variable rather than semilatus rectum). These were then converted into classical orbital element curves and plotted.

Table 5 Equinoctial Orbital Element Coefficients, $T/m_0 = 10^{-1}$ N/kg

$y = c_1t^6 + c_2t^5 + c_3t^4 + c_4t^3 + c_5t^2 + c_6t + c_7$								
y	c₁	c₂	c₃	c₄	c₅	c₆	c₇	R²
<i>a</i>/R_{Earth}	0	0	0	0.0004	0.0052	0.1219	1.0783	0.9997
<i>f</i>	0	0	0	4×10^{-17}	-4×10^{-17}	3×10^{-16}	3×10^{-16}	0.9999
<i>g</i>	0	0	-9×10^{-5}	0.0022	-0.0107	0.0285	-0.007	0.9999
<i>h</i>	0	1×10^{-18}	-3×10^{-17}	2×10^{-16}	-8×10^{-16}	1×10^{-15}	-3×10^{-16}	0.9994
<i>k</i>	0	0	7×10^{-5}	-0.0012	0.0076	-0.0114	0.2601	0.9988

To provide a better physical sense of the results, the equinoctial elements and their associated curves are converted into classical orbital elements. Figures 12, 13, and 14 show a comparison of the time history of the semimajor axis, eccentricity, and inclination with ω_{initial} : 0° , 90° , 180° , and 270° . Furthermore, figures 15-19 show the results for the equinoctial orbital elements. Figure 12 shows how ω_{initial} has no effect on the solution provided by SEPSHOT. The curves for ω_{initial} : 0° , 90° , 180° , and 270° are superimposed and fit perfectly on top of each other. This indicates that SEPSHOT's solution isn't dependent on ω_{initial} .

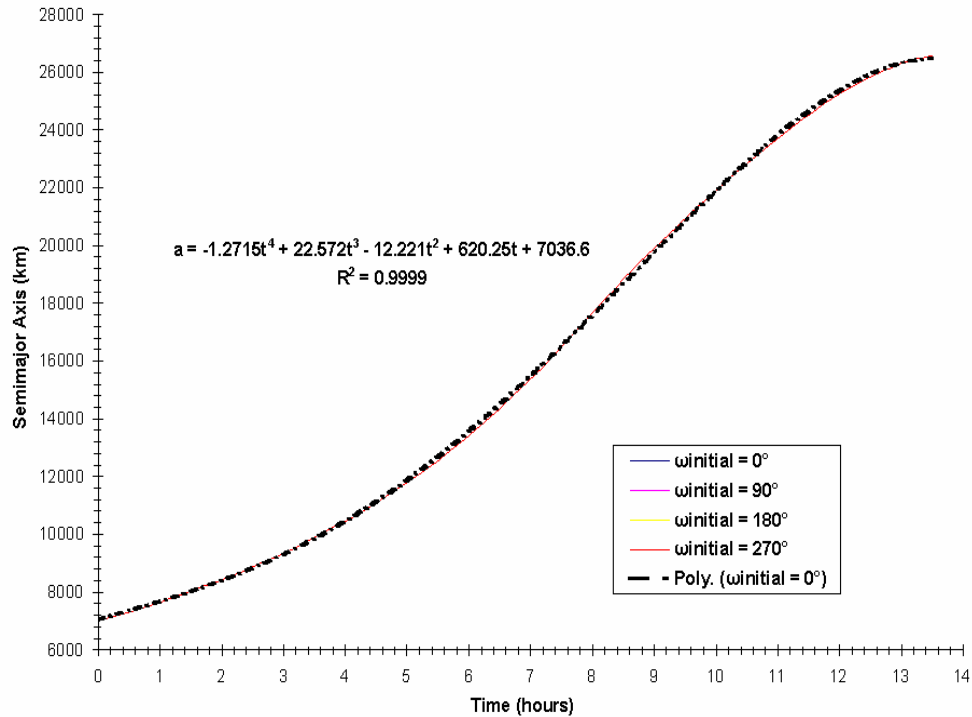


Figure 12: Semimajor Axis Time History, $T/m_0=10^{-1}$ N/kg

Figure 13 depicts how eccentricity is independent of ω_{initial} . The curves for ω_{initial} : 0° , 90° , 180° , and 270° are identical. Again, this demonstrates that SEPPOT's solution is independent of ω_{initial} . The trendline for this figure also seems to be very accurate since its determination coefficient has a value close to 1.

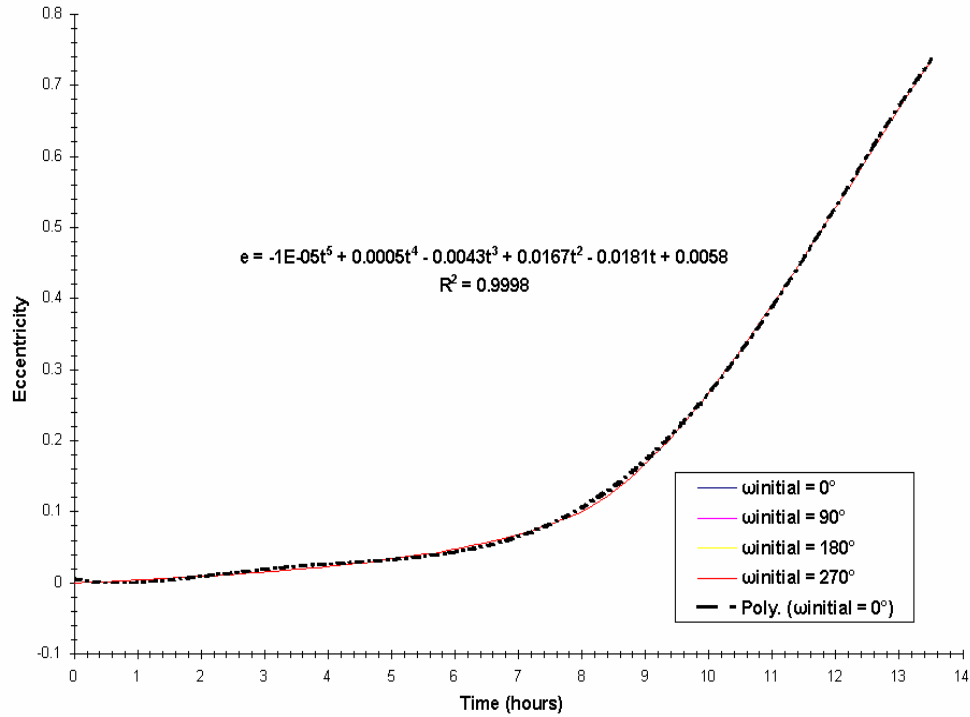


Figure 13: Eccentricity Time History, $T/m_0=10^{-1}$ N/kg

Figure 14 supports what Figures 12 and 13 indicate, that SEPSOT's solution is independent of ω_{initial} . Furthermore, the trendline for this case consists of a third order polynomial and is a perfect match to the actual data since the determination coefficient is equivalent to 1.

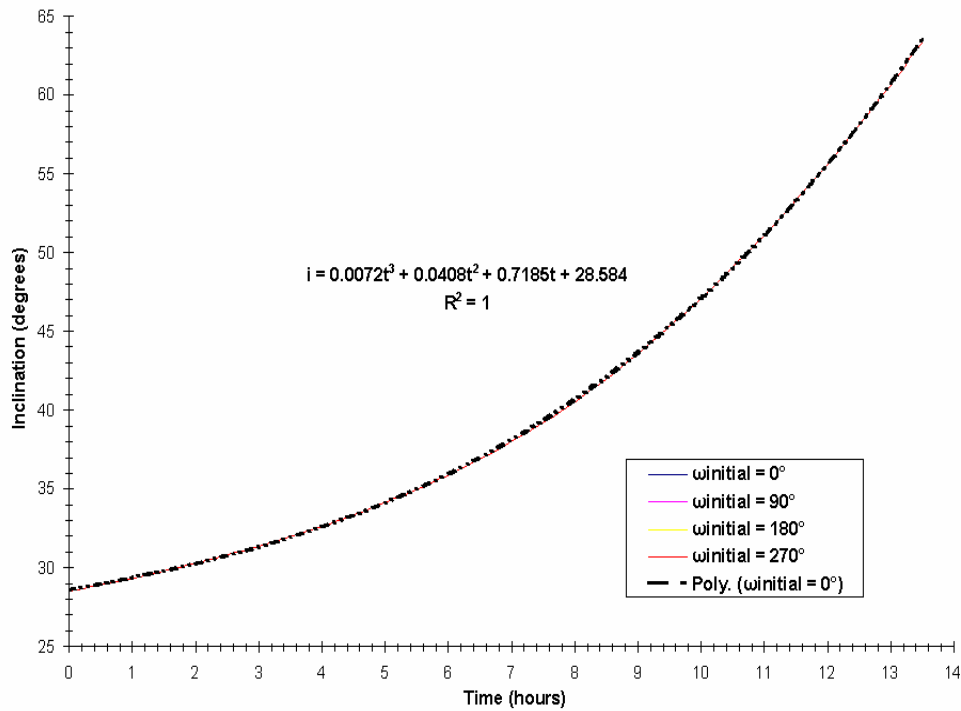


Figure 14: Inclination Time History, $T/m_0=10^{-1}$ N/kg

The analytical analysis conducted for the $T/m_0 = 10^{-2}$ N/kg case consists on deriving the polynomial equations for the time history of the semimajor axis, eccentricity, inclination, and equinoctial orbital elements (a , f , g , h , and k). Refer to Table 6 for a comparison of the coefficients of the polynomial equation derived for each equinoctial orbital element.

Table 6: Time History Coefficients, $T/m_0 = 10^{-2}$ N/kg

$y = c_1t^6 + c_2t^5 + c_3t^4 + c_4t^3 + c_5t^2 + c_6t + c_7$								
y	c_1	c_2	c_3	c_4	c_5	c_6	c_7	R^2
a/R_{Earth}	0	0	0	4×10^{-7}	6×10^{-5}	0.0119	1.0792	0.9998
f	4×10^{-29}	-2×10^{-26}	3×10^{-24}	-2×10^{-22}	3×10^{-21}	5×10^{-20}	-3×10^{-19}	0.9989
g	0	0	-9×10^{-9}	2×10^{-6}	-0.0001	0.0029	-0.0078	0.9999
h	6×10^{-29}	-2×10^{-26}	2×10^{-24}	-1×10^{-22}	4×10^{-21}	-5×10^{-20}	8×10^{-20}	0.9968
k	0	0	6×10^{-9}	-1×10^{-6}	7×10^{-5}	-0.0011	0.2605	0.9987

Figures 15-17 depict a comparison between the trendlines and the actual data for the semimajor axis, eccentricity, and inclination.

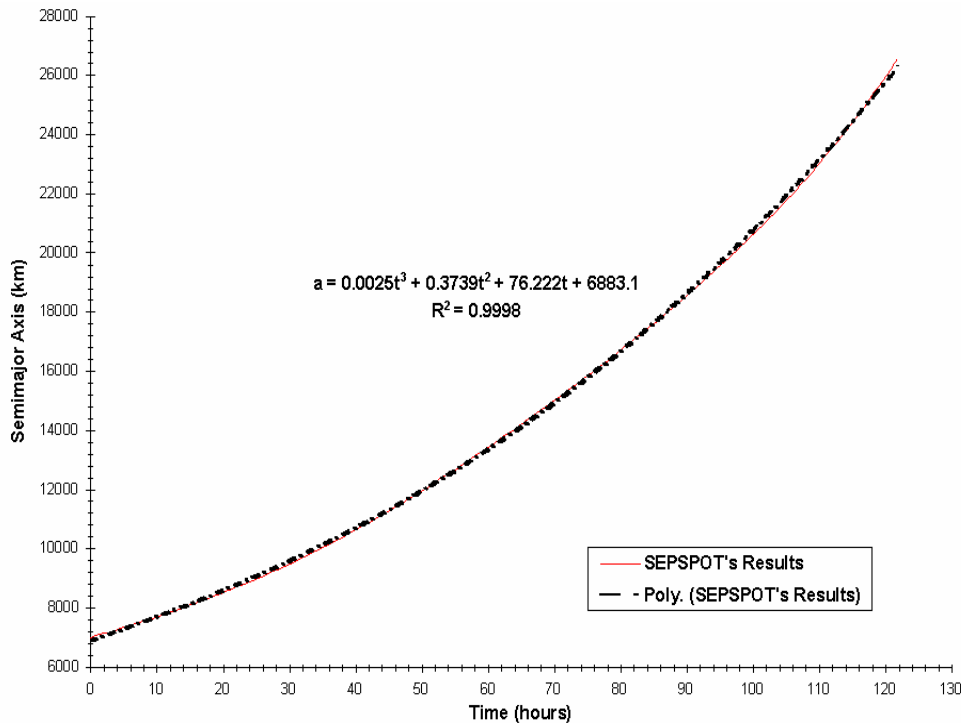


Figure 15: Semimajor Axis Time History, $T/m_0 = 10^{-2}$ N/kg

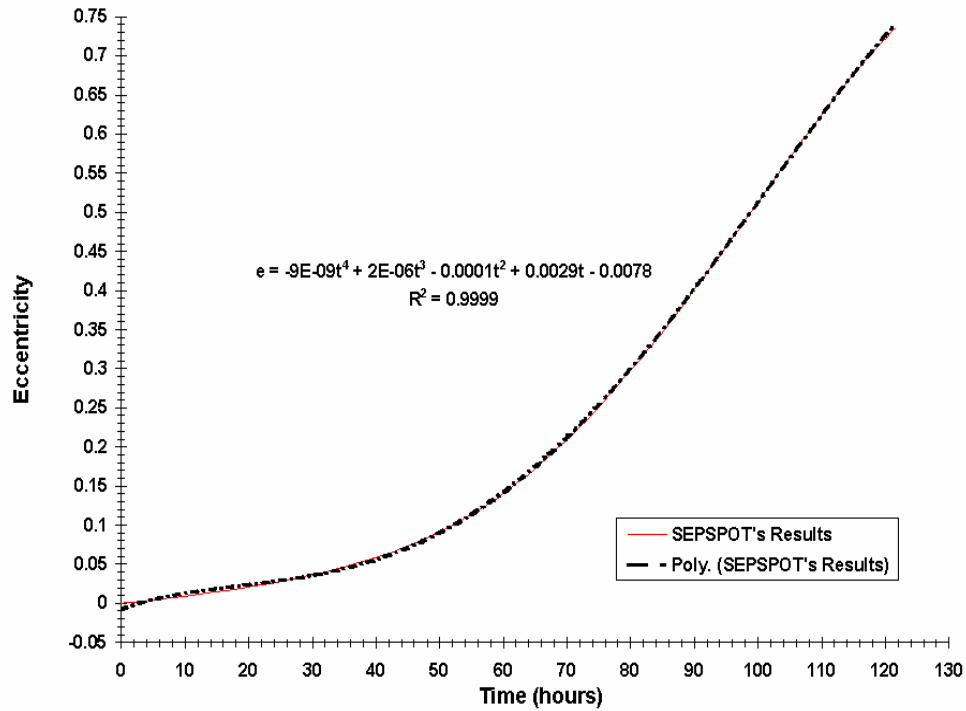


Figure 16: Eccentricity Time History, $T/m_0 = 10^{-2}$ N/kg

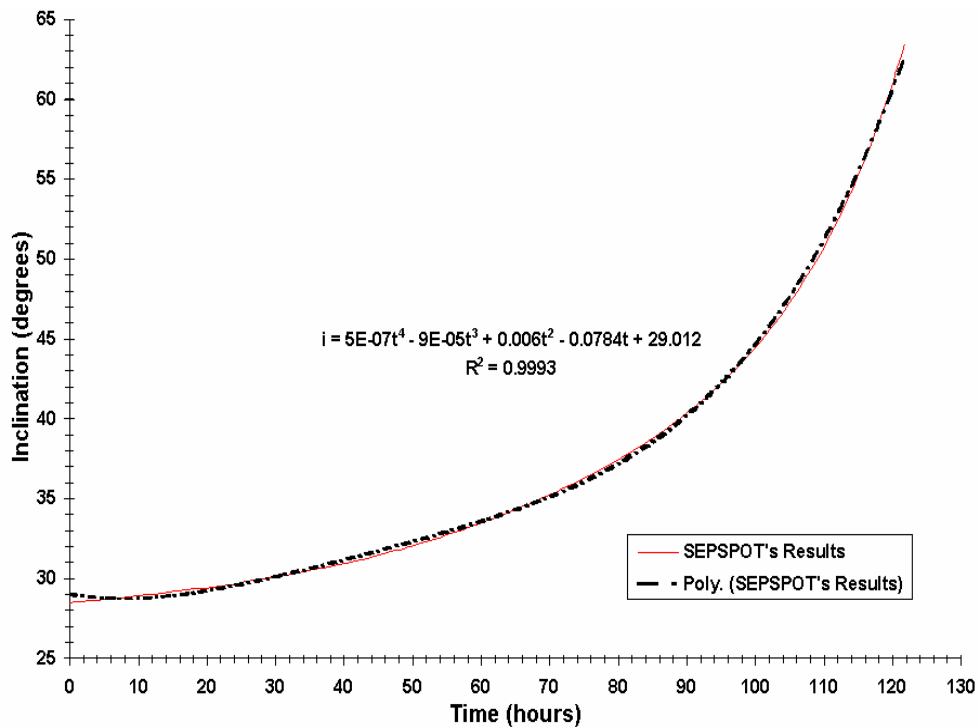


Figure 17: Inclination Time History, $T/m_0 = 10^{-2}$ N/kg

VII. Conclusions

A comparison between Spencer's analytical data and SEPSOT's numerical data showed that the percent error between the two is small, there is about a 13% percent difference for the initial

thrust acceleration of 10^{-1} N/kg and 10^{-2} N/kg. The factor that affected the results of both solutions is that for Spencer's analytical solution the radius of perigee was held constant while with SEPSOT's numerical solution the radius of perigee was free. This difference indicates that while Spencer's solution was closely related to SEPSOT's solution it can be improved by doing another analytical analysis with the radius of perigee free.

Overall, all the polynomial equations derived for the initial thrust acceleration of 10^{-1} N/kg and 10^{-2} N/kg were extremely accurate since the threshold for the determination coefficient was 0.995. The small discrepancies between the trendlines and some of the actual data are the result of computer precision.

References

- ¹ Herman, A.L. and Spencer, D.B., "Optimal, Low-Thrust Earth-Orbit Transfers Using Higher-Order Collocation Methods," *Journal of Guidance, Control, and Dynamics*, Vol. 25, No. 1, 2002, pp.40-47.
- ² Bruschi, R.G., and Vincent, T.L., "Low-Thrust, Minimum Fuel, Orbit Transfers," *Acta Astronautica*, Vol. 16, No. 2, 1971, pp.65-73.
- ³ Edelbaum, T.N., "Propulsion Requirements for Controllable Satellites," *ARS Journal*, Vol. 32, No. 8, 1961, pp.1079-1089.
- ⁴ Redding, D.C., "Optimal Low-Thrust Transfers to Geosynchronous Orbit," Stanford Univ. Guidance and Control Lab., Rept. SUDAAR 539, Stanford, CA, Sept. 1983.
- ⁵ Herman, A.L., and Conway, B.A., "Optimal, Low-Thrust, Earth-Moon Orbit Transfer," *AIAA Journal of Guidance, Control, And Dynamics*, Vol. 21, No. 1, January-February, 1998, pp. 141-147.
- ⁶ Prussing, J.E., "A Class of Optimal Two-Impulse Rendezvous Using Multiple-Revolution Lambert Solutions," *The Journal of the Astronautical Sciences*, Vol. 48, Nos. 2 and 3, April-September, 2000, pp. 131-148.
- ⁷ Kechichian, J.A., "Minimum-Time Low-Thrust Rendezvous and Transfer Using Epoch Mean Longitude Formulation," *Journal of Guidance, Control, and Dynamics*, Vol. 22, No. 3, May-June, 1999, pp. 421-432.
- ⁸ Coverstone-Carroll, V. and Williams, S.N., "Optimal Low Thrust Trajectories Using Differential Inclusion Concepts," *The Journal of the Astronautical Sciences*, Vol. 42, No. 4, October-December, 1994, pp. 379-393.
- ⁹ Betts, J.T., "Optimal Interplanetary Orbit Transfers by Direct Transcription," *The Journal of the Astronautical Sciences*, Vol. 42, No. 3, July-September, 1994, pp. 247-268.
- ¹⁰ Kechichian, J.A., "Optimal Low-Earth-Orbit-Geostationary-Earth-Orbit Intermediate Acceleration Orbit Transfer," *Journal of Guidance, Control, and Dynamics*, Vol. 20, No. 4, July-August, 1997, pp. 803-811.
- ¹¹ Spencer, D.B., "An Analytical Solution Method For Near-Optimal, Continuous-Thrust Orbit Transfers", Ph.D. Dissertation, University of Colorado, January 1994.
- ¹² Sackett, L.L., Malchow, H.L., and Edelbaum, T.N., Solar Electric Geocentric Transfer with Attitude Constraints: Program Manual. The Charles Stark Draper Laboratory, Inc., August, 1975.
- ¹³ Sackett, L.L., Malchow, H.L., and Edelbaum, T.N., Solar Electric Geocentric Transfer with Attitude Constraints: Analysis. The Charles Stark Draper Laboratory, Inc., August, 1975.
- ¹⁴ Jahn, R.G., Physics of Electric Propulsion. New York: McGraw-Hill Book Company, 1968.